Fusion Engineering and Design 230 (2026) 115870

Contents lists available at ScienceDirect

Fusion Engineering and Design

journal homepage: www.elsevier.com/locate/fusengdes

Concept design and integration of Volumetric Neutron Source upper port shield plug

Vincenzo Claps [a,*], Ivo Moscato [b,c], Eugenio Vallone [c], Giuseppe Nicolò [c], Marco Passarello [c], Pietro Alessandro Di Maio [c], Christian Bachmann [b], Rocco Mozzillo [a]

[a] CREATE, Engineering Department of Basilicata University, Campus Macchia Romana (PZ) 85100, Italy
[b] EUROfusion Consortium, FTD Department, Garching, Boltzmannstr. 2, Germany
[c] Department of Engineering, University of Palermo, Viale delle Scienze, Ed. 6, Palermo 90128, Italy

ARTICLE INFO

Keywords:
VNS
Remote maintenance
Shield plug
Design integration
CAD

ABSTRACT

The Volumetric Neutron Source project, launched in 2023, primarily aims to test major in-vessel components within a new test facility based on the tokamak configuration. During the project's preliminary study phase, particular attention is also given to remote maintenance aspects, which are influencing and contributing to the definition of the in-vessel components design and the overall machine layout.

The Shielding Blanket is assumed to be replaced via Upper Port, which is equipped with a Shield Plug and all the necessary services for feeding the blanket segments. The Shield Plug plays a fundamental role in protecting the Upper Port from neutron and thermal hazards, thus reducing the exposure of external structures to radiation and limiting the thermal load on surrounding elements. The design of the Shield Plug must balance both structural and functional requirements, while at the same time ensuring ease of removal and reinstallation during remote maintenance operations. For this reason, particular attention is paid to the design of this component.

The current work focused on the design and integration of the Upper Port Shield Plug structure, preliminary structural analysis has been also carried out to check the structural integrity of the Shield Plug against the most severe loads. The conceptual design of the Shield Plug and the results of the structural analysis are here presented.

1. Introduction

The Volumetric Neutron Source (VNS) is a compact beam-driven tokamak concept aimed at providing a high 14 MeV neutron flux to test and qualify fusion nuclear components, with a primary focus on breeding blanket (BB) systems and with the purpose of addressing potential showstoppers [1,2]. The project also directly addresses key nuclear-facility aspects such as remote maintenance, tritium management and plant integration, in order to build operational experience relevant to future fusion power plants. In this framework, the upper ports play a key role, as they facilitate the replacement of internal components, such as the shielding blanket [3], through remote operations. In the conceptual phase of design, remote handling (RH) is identified as a key factor. This is due to the periodic replacement of components inside the vacuum vessel to the active maintenance facility (AMF). This procedure is undertaken using sealed casks and dedicated equipment [3].

The upper ports are equipped with dedicated port components, including a shield plug and service routing that is required to feed the blanket segments. The shield plug is therefore a key safety and integration component, since it must restore the shielding function locally in place of the vacuum vessel shielding across the port opening, while simultaneously enabling service routing and maintainability. This paper summarizes the ongoing design activity on the VNS **Upper Port Shield Plug** (UPSP), covering the design concept, integration features, and a preliminary structural verification based on preliminary and simplified Finite Element Modelling (FEM) and thermal-hydraulic modelling (CFD) activity, included as a dedicated section.

2. Upper port shield plug functional requirements

The current maintenance strategy for in-vessel components, such as the Shielding Blanket, is predicated on their removal through the upper ports and on the utilization of dedicated robotic systems and

* Corresponding author.
E-mail address: vincenzo.claps@unibas.it (V. Claps).

https://doi.org/10.1016/j.fusengdes.2026.115870
Received 31 December 2025; Received in revised form 4 June 2026; Accepted 5 June 2026
Available online 10 June 2026

transporters to perform remote maintenance operations, given that the areas are inaccessible to workers due to the high level of radiological activation [1,2]. From the current concept definition, the UPSP shall:

- **Provide neutron and gamma shielding** of the upper port region, effectively replacing the shielding function locally where the vacuum vessel is interrupted by the port opening.
- **Accommodate blanket service** pipes through the port region and support the installation and alignment of the pipe forest, including dedicated centering or alignment features.
- Provide **vertical structural support** to blanket segments.
- Be **compatible with remote handling tools**, enabling removal and reinstallation during maintenance operations.

In order to ensure that these requirements are met, it is essential to respect the structural limits under representative loads, which include gravity and pressurized cooling circuits. Furthermore, it is necessary to ensure maintainability and integration compatibility with adjacent Upper Port structures, Fig. 1.

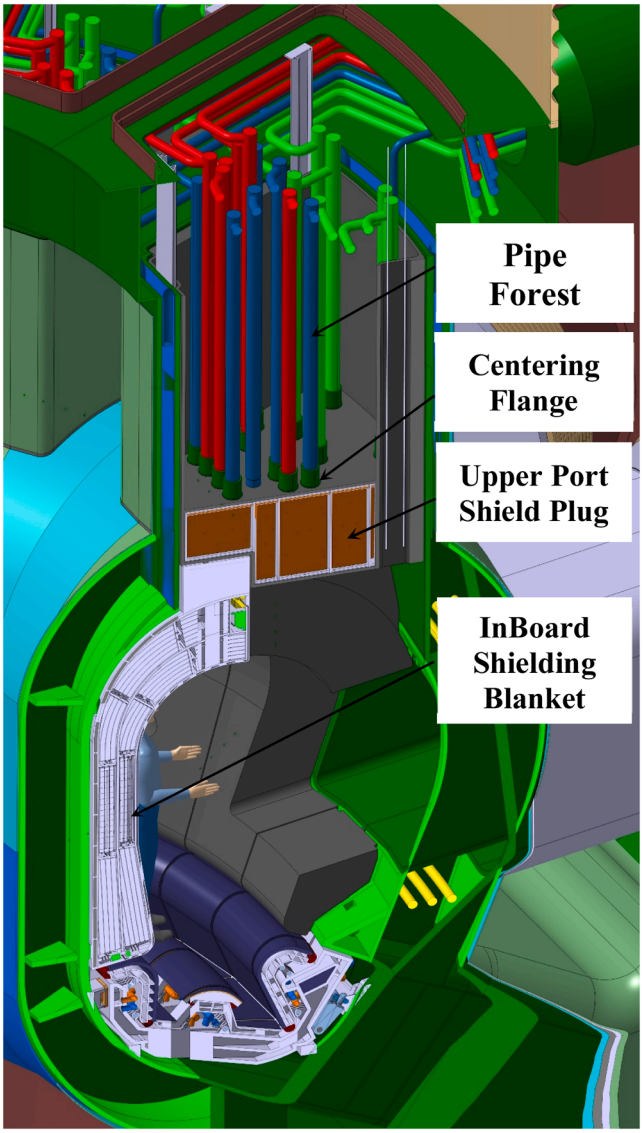

Figure 1. Cross section overview of Upper Port Shielding Plug inside the VV.

2.1. Integration with remote handling operations

The design of the UPSP and its interfaces with surrounding upper port components are strongly influenced by remote handling requirements. In VNS, the SB segments are extracted through upper ports by means of vertical transporters and transferred to the AMF in sealed casks. This ensures double confinement, thereby mitigating the spread of radioactive dust and tritium outgassing when the upper port is opened. In order to ensure the efficacy of a consistent maintenance sequence, it is necessary to remove the components in the following order [4–7]:

1. Bio-shield roof concrete plugs;
2. VV closure plate;
3. pipe top caps;
4. in-bore cutting/welding at SB chimney level [5,6];
5. ex-bore cutting at horizontal leg;
6. pipe forest transfer in a dedicated cask;
7. Upper Port Shield Plug removal;
8. SB replacement [3,4];

Perform the reverse sequence for reinstallation, welding and leak testing.

Pipe cutting and welding operations in the upper port region are expected to take place in a comparatively low gamma-radiation environment (below about 1 Gy/h), since the weld locations are situated at the backside of the blanket while the blanket segments remain in place. Under these conditions, radiation from the highly activated first wall can reach the tools mainly through the gaps between adjacent blankets. To preserve the reweldability of previously neutron-irradiated pipes, a dedicated design target of 1 appm helium production has been adopted for the cutting and rewelding locations in the in-vessel component cooling pipes. Since these locations are additionally protected by the shielding blanket and chimney structures, the actual helium production is expected to remain below this limit [8]. The final positioning of the weld locations will nevertheless be supported by dedicated local neutronics and activation assessments to confirm both the shutdown dose rates and the reweldability margins.

3. Upper port shield plug design

The Upper Port Shield Plug, (Fig. 2), consists of a box-shaped structural body made of AISI 316L(N)-IG stainless steel. It is located in the upper port region and attached to the port structures through dedicated side flanges placed on its sidewalls. A further UPSP interface with the upper port is provided by the presence of three permanent rails. These are utilized by the robotic system for blanket replacement purposes. The design is organized into functional zones:

- The **upper structural region is responsible** for providing stiffness and interfaces with the vacuum vessel.

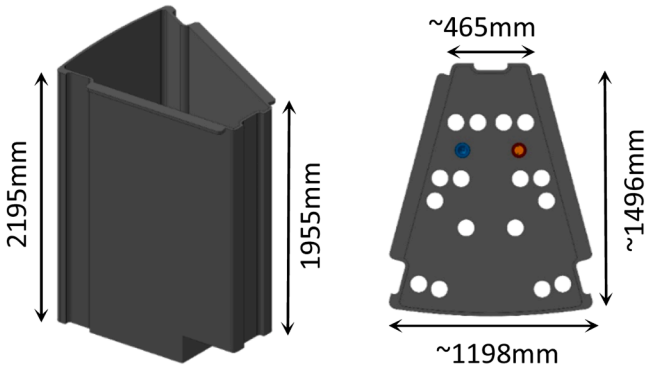

Figure 2. Upper Port Shield Plug Overview.

- The **lower shielding region** has been designed as a closed volume, with the function of hosting the shielding medium and the integrated cooling solution.

3.1. Shielding concept and cooling integration

The shielding section, which constitutes the lower part of the structure, is a closed box volume that is filled with shielding material, which may take the form of metallic or ceramic pebbles. This solution facilitates the attenuation of neutrons through a dense, fillable medium, while concurrently enabling active cooling mechanisms. The pebbles region is designed to be actively cooled by pressurized sub-cooled water, which is integrated into the structure via internal sub-volumes/boxes and collectors. The aim of this integration is to achieve a more uniform coolant distribution within the shielding volume and to limit local temperature gradients.

A first mass budget was derived from the current geometry and assumptions:

- Structural mass: **2732 kg**.
- Pebbles mass: **5341 kg**.
- Assumed packing factor: **0.625**.
- Assumed density (reference value): **7850 kg/m^3**.
- Total UPSP mass: ~**8073 kg**.

These values are important not only for structural sizing but also for defining remote handling constraints, lifting scenarios, and interface loads transmitted to the port structures.

3.2. Pipe forest routing and alignment features

The UPSP accommodates service pipes for blanket segments and supports the installation phase of the pipe forest. The alignment of the pipe is ensured through the use of dedicated centering flanges, Fig. 3, which maintain the pipe's position and reduce the accumulation of assembly tolerances along the port depth. It is posited that such centering features may also represent a potential mitigation measure to reduce neutron streaming through gaps. However, it must be noted that their implementation requires sufficient available space within the port envelope.

3.3. Vertical supports for blanket segments

The UPSP concept integrates vertical support features into the port plug, with the objective of carrying blanket segment loads and contributing to stability and repeatability during the installation and removal phases.

The loads transmitted from the blanket are transferred via these supports to the port plug and vacuum vessel structures, Fig. 4.

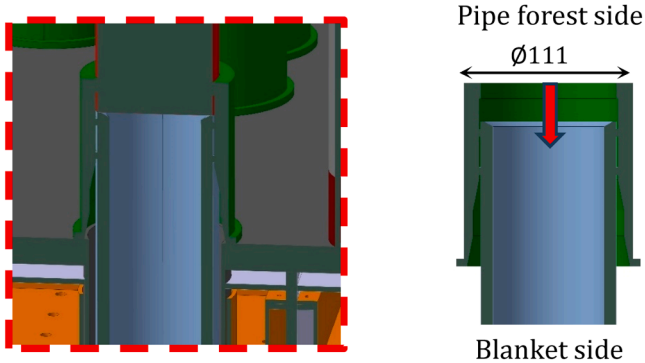

Figure 3. Centering Flange Overview.

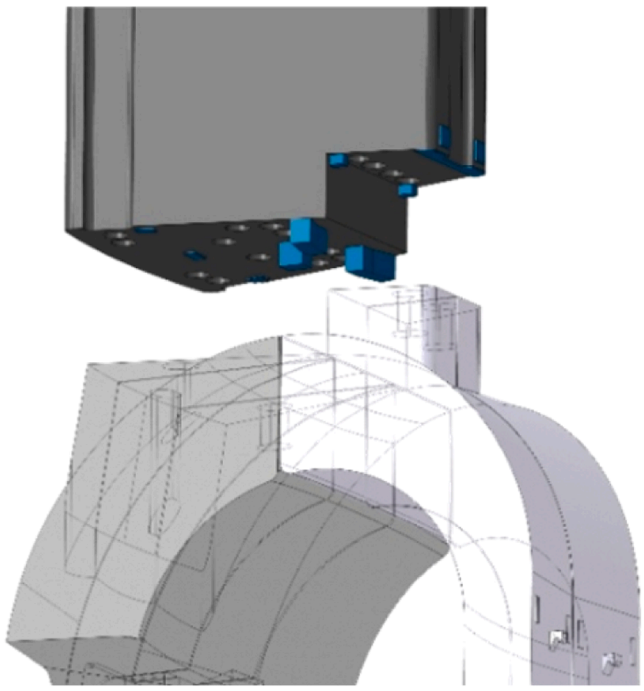

Figure 4. Vertical supports of the blanket segments integrated into the port plug.

These supports are composed of simple steel pads that are fully welded to the port plug structure. Specifically, the supports integrated into the UPSP structure include, Fig. 5:

1. Radial supports for the port plug at both the inboard and outboard walls. (1).
2. Radial supports for the outboard blanket segments. (2).
3. A shear key for the central outboard segment serving as toroidal support. (3).
4. Upper vertical supports for the outboard blanket segments. (4).
5. Upper vertical supports for the inboard shielding blankets. (5).
6. Recesses for the blankets service pipes. (6).
7. A shear key for the inboard segment serving as toroidal support. (7).

4. Structural model and preliminary FEM analysis

4.1. Modelling approach and assumptions

A preliminary linear elastic shell finite element model was developed for the UPSP. The material utilized is AISI 316L(N)-IG, and the analysis is conducted with the objective of assessing the structural response under conservative representative loads and identifying the most critical regions. This information is then used to guide design iteration. The most relevant simplifying assumptions at this stage are as follows:

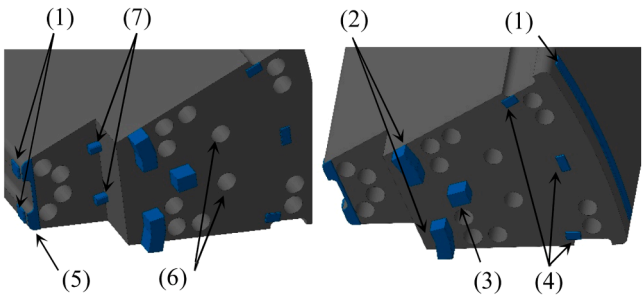

Figure 5. SB segment support scheme integrated on the port plug.

- Shell idealization of the box plates;
- Linear elastic material behaviour;
- Load cases focusing on severe combinations for the box region, including internal pressure for cooling circuits and gravity contributions.

A representative operating condition used in the preliminary verification included:

$$\begin{cases} \mathbf{p_{int}} = 2MPa \\ \mathbf{T_{op}} = 50^{\circ}C \end{cases} \quad (1)$$

4.2. Stress classification and acceptance criteria

Post-processing followed an approach consistent with RCC-MRx stress categorization, with stress components classified for Level A criteria. The verification focused on **Type P** damage prevention, using criteria on primary membrane stress and combined primary membrane + primary bending stress:

$$\overline{P_m} \leq S_m(\vartheta_m) \quad (2)$$

$$\overline{P_m} + P_b \leq 1.5\ S_m(\vartheta_m) \quad (3)$$

4.3. Preliminary results and key outcomes

The preliminary results indicate that both the primary membrane stress and the combined primary membrane + primary bending stress satisfy the adopted Level A acceptance criteria for the assessed thicknesses (20 mm and 25 mm), as summarized in Table 1. As anticipated, an increase of the external shell thickness resulted in an improvement of the structural margin. The structural margin is here expressed by the margin of safety:

$$MS = \frac{S_m(\vartheta_m)}{\overline{P_m}} - 1;\ MS = \frac{1.5\ S_m(\vartheta_m)}{\overline{P_m} + P_b} - 1 \quad (4)$$

The key stress maps are reported in Fig. 6 and Fig. 7.

4.4. Design iteration

The outcomes indicate that the concept is broadly viable in terms of global structural sizing. The present FEM assessment considers normal operating loads only. Additional load cases such as electromagnetic loads must be considered in the next steps, too. Further design iterations will focus on improving structural robustness and margin, and on consolidating the modelling assumptions and load cases. The next design steps that have been identified are as follows:

- assessment of potential local reinforcements/stiffening strategies in critical regions, if required by extended load cases or interface refinements;
- moving beyond linear screening to non-linear procedures (e.g., limit analysis) to better quantify margin and redistribution effects;
- refinement of boundary conditions and interface modelling to represent the load transfer to side flanges and vacuum vessel structure more realistically.
- extension of the structural assessment to the definition of the design driving load cases, particularly blanket support reactions, electromagnetic loads during disruption events, and seismic conditions;

Table 1
FEM results overview.

External shell THK [mm]	P_m [MPa]	MS	P_m+P_b [MPa]	MS
20	122 < 138	13%	199 < 207	4%
25	102 < 138	35%	150 < 207	38%

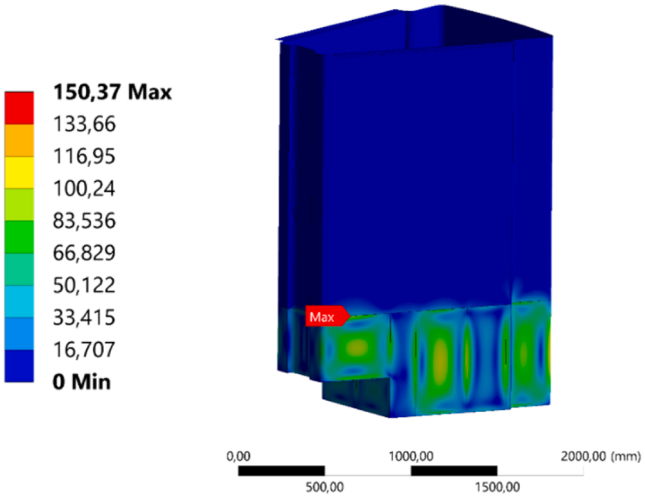

Figure 6. Bending + Membrane Stress [MPa] - $Shell_{THK}$=25mm.

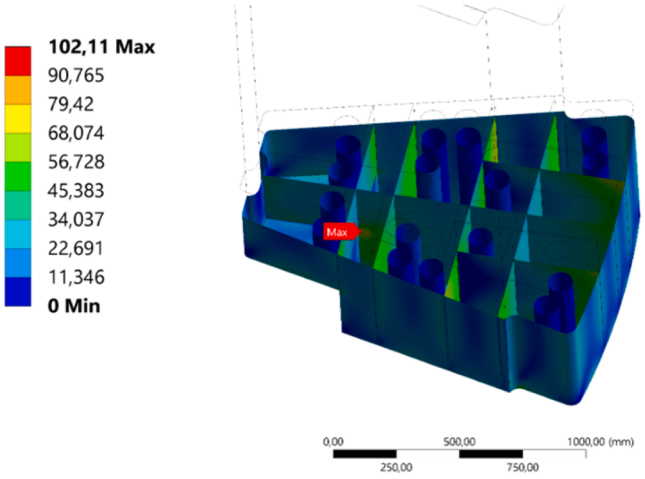

Figure 7. Primary Membrane Stress [MPa] – $Shell_{THK}$=25mm.

- evaluation of the UPSP behaviour under machine state dependent Upper Port interface displacements, to support the identification of the governing load combinations.

5. Thermal-Hydraulic modelling (CFD)

The steady-state hydraulic performances of the Shield Plug cooling circuit have been assessed in terms of coolant pressure distribution, total pressure drop and coolant mass flow rate distribution, in order to verify whether the shield plug cooling circuit is capable of providing adequate and uniform cooling to all solid parts of the component.

To this end, a 3D-CFD isothermal analysis has been performed under steady-state conditions using the commercial CFD code ANSYS-CFX 2023 R2 [9].

5.1. The shield plug cooling circuit

The Shield Plug cooling circuit is fed by pressurized subcooled water under the conditions shown in Table 2.

The cooling layout is designed to promote a uniform coolant distribution among the shielding boxes, with the aim of limiting temperature gradients and associated thermal stresses under normal operating conditions. At this stage, the mass flow rate is based on hydraulic considerations, namely to ensure a minimum coolant velocity within the

Table 2
Coolant thermodynamic inlet conditions.

Parameter	Value
p_{in} [MPa]	1.0
T_{in} [°C]	50
G [kg/s]	10

circuit.

The shielding boxes are shown in the top right corner of Fig. 8.

The coolant enters the inlet manifold located at the top of the component (right side of Fig. 9) and is distributed through a grid towards the upper distribution plate (left side of Fig. 8). This plate directs the flow to the outermost region of the component, from where it proceeds to the lower distribution plate. The lower plate ensures an even distribution of coolant among the shielding boxes. The fluid enters each shielding box through dedicated distribution holes (bottom left corner of Fig. 9), designed to promote uniform flow and prevent preferential paths between the shielding pebbles. Inside the shielding boxes, the coolant flows poloidally from bottom to top, removing the deposited thermal power, and finally reaches the upper collection plate, which channels it towards the outlet manifold (see Fig. 9).

A gap is provided between the outer walls of the shielding boxes and the structure of the UPSP, allowing the boxes containing the shielding pebbles to be inserted into the UPSP. Under normal operating conditions, this gap is crossed by a portion of the coolant that bypasses the shielding boxes and therefore does not contribute to their cooling. The estimation of this bypass is a key feedback for the design of the shield plug cooling system.

5.2. CFD analysis setup

The hydraulic performances of the Shield Plug cooling circuit have been evaluated by performing an isothermal CFD analysis under steady-state conditions, based on the coolant operating conditions shown in Table 2.

The adopted discretisation, as well as the models, assumptions and boundary conditions, have been selected in analogy with previous work carried out by the UNIPA thermal-hydraulic research group [10–12].

Particular attention has been devoted to the modelling of the region containing the shielding pebbles. Due to the inherent geometric complexity of the pebble arrangement, a detailed representation has been deemed impractical, as it would have significantly hindered the simulation of the entire coolant domain. Consequently, the pebble region has been modelled using a porous media approach, which effectively accounts for their presence while ensuring computational feasibility.

In particular, the Ansys CFX software allows an isotropic pressure loss per unit length (S_p) to be defined within a porous domain as a function of the dynamic pressure head $\left(\rho\frac{u^2}{2}\right)$ through a loss coefficient

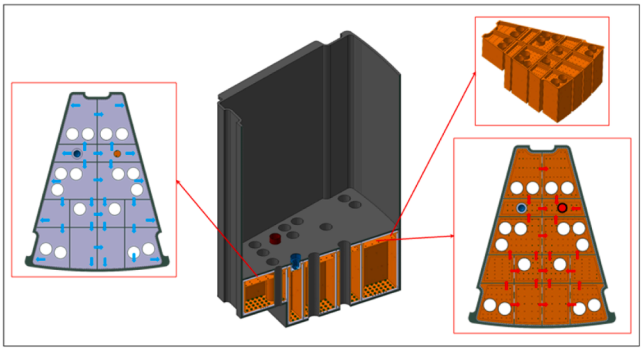

Figure 8. Shielding boxes and coolant distribution and collection plates.

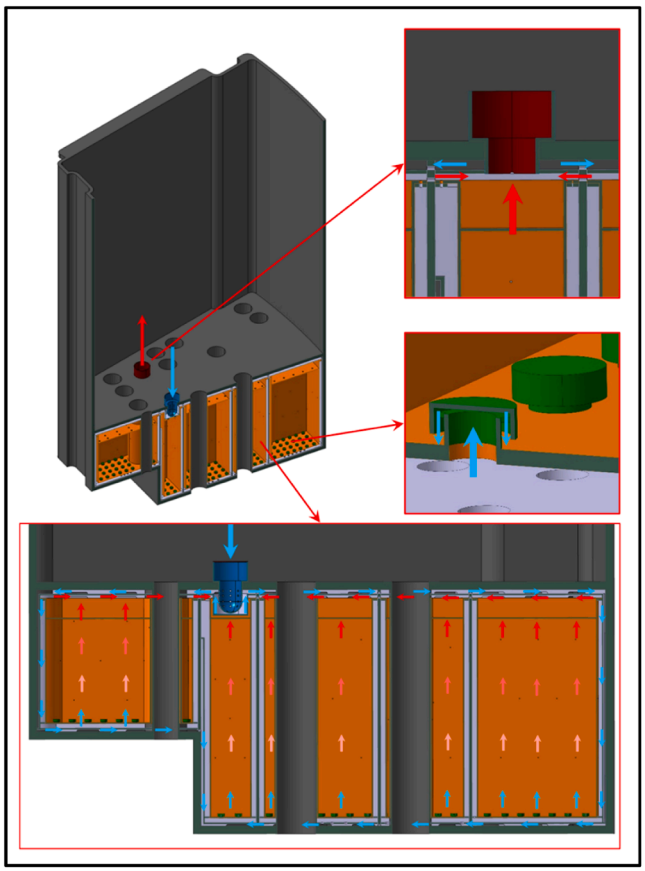

Figure 9. Shield plug cooling scheme.

(K_{loss}) according to the well-known formula [9]:

$$S_p = K_{loss}\rho\frac{u^2}{2} \tag{5}$$

On the other hand, the pressure drop (Δp) through a pebble bed of height H can be described by the equation [13]:

$$\Delta p = \psi\left(\frac{H}{d_h}\right)\rho\frac{u_p^2}{2} \tag{6}$$

Where ψ is the pressure drop coefficient, ρ is the fluid density, and u_p is the mean velocity in the gaps between particles.

To relate these quantities to measurable parameters, the void fraction ε can be introduced, defined as $\varepsilon = 1 - \frac{V_s}{V}$ where V_s is the volume occupied by the pebbles and V is the total volume. The hydraulic diameter d_h relates to pebbles diameter d and the void fraction via the equation:

$$d_h \sim d\frac{\epsilon}{1-\epsilon} \tag{7}$$

Furthermore, the superficial velocity u (based on the empty cross-section) is related to the interstitial velocity by:

$$u = \epsilon\, u_p \tag{8}$$

Substituting these definitions, the governing pressure drop equation becomes:

$$\Delta p = \psi\left(\frac{H}{d}\right)\left(\frac{1-\epsilon}{\epsilon^3}\right)\rho\frac{u^2}{2} \tag{9}$$

The pressure drop coefficient ψ can be expressed as a function of the Reynolds number $\left(Re = \frac{d\,u\,\rho}{\mu}\right)$ via the following equation [13] that

covers both laminar and turbulent regimes, valid up to $Re/(1-\epsilon) = 5{\cdot}10^4$:

$$\psi = \frac{320}{\frac{Re}{1-\epsilon}} + \frac{6}{\left(\frac{Re}{1-\epsilon}\right)^{0.1}} \tag{10}$$

Combining Eqs. (9) and (10), a loss coefficient per unit pebble-bed length (K_{loss}) can be easily derived as:

$$K_{loss} = \left(\frac{320}{\frac{Re}{1-\epsilon}} + \frac{6}{\left(\frac{Re}{1-\epsilon}\right)^{0.1}}\right)\left(\frac{1}{d}\right)\left(\frac{1-\epsilon}{\epsilon^3}\right) \tag{11}$$

It is worth highlighting that, in principle, the void fraction ϵ is not uniform throughout the bed [13]. Near the confining walls, the random packing is disrupted. The void fraction starts at $\epsilon = 1$ at the wall, reaches a minimum at a distance of d/2, and then oscillates with decreasing amplitude before settling to a bulk mean value $\epsilon_t \approx 0.375$ deeper in the bed.

Nevertheless, the effect of the wall on the overall fluid motion rapidly decreases with the ratio (D /d) [13] between the diameter of the box housing the pebbles and the diameter of the pebbles. Therefore, it has been assumed as a first approximation that the void fraction is uniform and equal to $\epsilon = 0.375$.

5.3. CFD analysis results

The steady-state hydraulic performances of the Shield Plug cooling circuit have been assessed in terms of total pressure distribution, total pressure drop and coolant mass flow rate distribution among the shielding boxes as well as coolant mass flow rate branching between the shielding boxes and their outer gaps.

The calculated total pressure drop (Δp_{TOT}) across the entire Shield Plug cooling circuit is approximately 0.11 MPa, with the majority of this loss occurring at the inlet distribution grid, as illustrated in Fig. 10. This behavior is consistent with the coolant velocity distribution shown in Fig. 11, where the maximum velocity (about 13.5 m/s) is observed at the inlet distribution grid. In contrast, coolant velocities remain significantly lower throughout the rest of the cooling domain.

Fig. 12 illustrates the mass flow rate distribution among the shielding boxes. The histogram clearly highlights a pronounced non-uniformity. In fact, while most shielding boxes exhibit flow rates in the range of approximately 0.15–0.30 kg/s, box No. 10 stands out with a peak value close to 0.75 kg/s, more than double the average (indicated by the red dashed line), likely due to its hydraulic proximity to the outlet manifold and, hence, reduced pressure losses compared to the others.

It is worth noting that the average line is reported only as a reference to quantify the degree of flow non-uniformity and does not represent a strict design requirement.

Table 3 shows the coolant mass flow rate branching between the shielding boxes and their outer gaps. Approximately 32.5% of the total flow (3.25 kg/s) is directed through the shielding boxes, while the remaining 67.5% (6.75 kg/s) bypasses them through the outer gaps. This

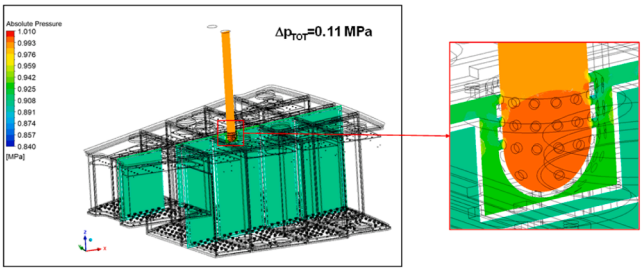

Figure 10. Coolant pressure field.

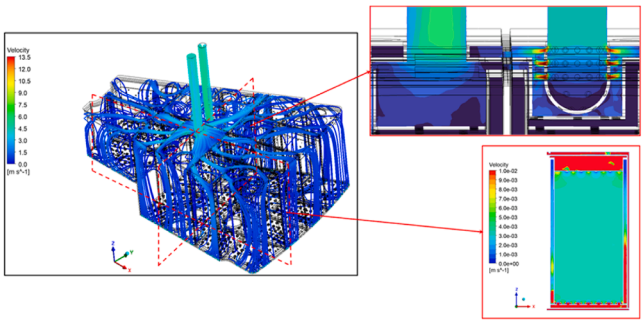

Figure 11. Coolant velocity field.

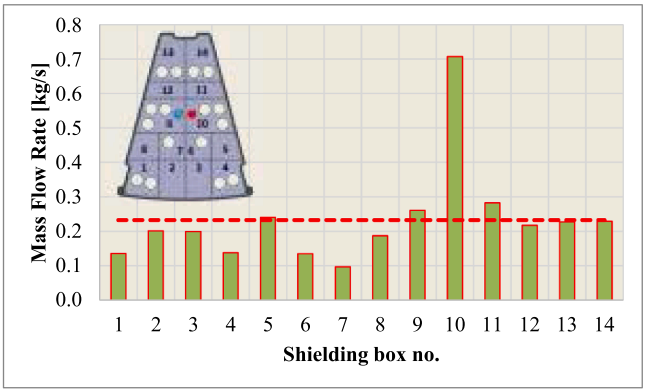

Figure 12. Mass flow rate distribution among shielding boxes.

Table 3
Mass flow rate branching between shielding boxes and outer gaps.

Domain	Mass Flow Rate [kg/s]
Shielding boxes	**3.25**
Outer gaps	**6.75**
Total	**10**

significant imbalance indicates a preferential flow path along the outer gaps, which must be addressed in future design iterations.

6. Conclusions and future work

A concept design for the VNS Upper Port Shield Plug has been developed, with particular emphasis placed on integration, shielding continuity, service routing, and remote maintenance compatibility. The proposed UPSP is a box-shaped AISI 316L(N)-IG structure with a pebble-filled, actively cooled shielding region, and dedicated features for pipe alignment (centering flanges) and blanket vertical support. Preliminary finite element analysis indicates that the design is promising from a global standpoint: primary membrane stresses and combined primary membrane + primary bending stresses meet the targeted acceptance criteria for the assessed thicknesses. This supports the viability of the current concept and motivates further optimization of load paths and structural robustness as the design and interfaces are consolidated. Future work will focus on:

- consolidating the structural layout by evaluating local reinforcements/stiffening options in critical regions.
- extension of the structural assessment to identify the load cases expected to drive the design, particularly those associated with blanket support reactions, disruption-induced electromagnetic loads, and seismic conditions.

- **refining the cooling circuit design** to improve overall hydraulic performance, building on the aspects highlighted by the CFD analyses.
- refining of remote handling interfaces and installation/removal sequences, consistent with the upper-port maintenance strategy in VNS.
- the UPSP's blanket vertical support function will be further consolidated through load assessments that include both blanket mechanical loads and electromagnetic loads during disruption events. This will enable verification and optimization of the support features.

CRediT authorship contribution statement

Vincenzo Claps: Writing – original draft, Visualization, Resources, Investigation, Formal analysis, Data curation, Conceptualization. **Ivo Moscato:** Validation, Supervision, Investigation, Conceptualization. **Eugenio Vallone:** Writing – original draft, Supervision, Data curation. **Giuseppe Nicolò:** Resources. **Marco Passarello:** Resources. **Pietro Alessandro Di Maio:** Supervision. **Christian Bachmann:** Visualization, Validation, Supervision, Project administration, Conceptualization. **Rocco Mozzillo:** Visualization, Validation, Supervision, Methodology, Conceptualization.

Declaration of competing interest

The authors declare that they have no known competing financial interests or personal relationships that could have appeared to influence the work reported in this paper.

Acknowledgments

This work has been carried out within the framework of the EUROfusion Consortium, funded by the European Union via the Euratom Research and Training Programme (Grant Agreement No 101052200 — EUROfusion). Views and opinions expressed are however those of the author(s) only and do not necessarily reflect those of the European Union or the European Commission. Neither the European Union nor the European Commission can be held responsible for them.

Data availability

Data will be made available on request.

References

[1] C. Bachmann, et al., Engineering concept of the VNS - a beam-driven tokamak for component testing, Fusion Eng. Des. 211 (2025) 114796.
[2] C. Bachmann, et al., Progress in the concept development of the VNS – a beam-driven tokamak for component testing, in: Proceedings of the 30th IAEA Fusion Energy Conference (FEC 2025), Chengdu, China, 2025. Contribution ID 36258 (conference pre-print /poster TEC-FNT).
[3] R. Mozzillo, et al., Remote maintenance strategy of the volumetric neutron source shielding blanket, Fusion Eng. Des. 218 (2025) 115226.
[4] R. Mozzillo, et al., Replacement strategy of the EU-DEMO and CFETR breeding blanket pipes, Fusion Eng. Des. 202 (2024) 114311.
[5] V. Claps, et al., Development of an In-bore welding tool prototype for DEMO's in-vessel pipes, Fusion Eng. Des. 217 (2025) 115166.
[6] D. Sorgente, et al., Overview of in-bore pipe cutting and welding tools for the maintenance of CFETR and EU DEMO, Fusion Eng. Des. 202 (2024) 114478.
[7] D. Sorgente, et al., Advancements of testing activities for development of in-bore welding tool for large feeding pipes of in-vessel components, Fusion Eng. Des. 220 (2025) 115367.
[8] C. Bachmann, "Facility description document (FDD)", EUROfusion,- doc. Ref. EFDA_D_2QK6DY, IDM UID:2QK6DY, v1.3, signed, Sep. 16, 2024.
[9] ANSYS Inc., "ANSYS CFX-solver theory guide," Release: 2023 R2, 2023.
[10] F.M. Castrovinci, et al., Thermofluid-dynamic assessment of the dual cooling scheme EU-DEMO divertor cassette, Fusion Eng. Des. 214 (2025) 114903.
[11] P.A. Di Maio, et al., Thermofluid-dynamic and thermal–structural assessment of the EU-DEMO WCLL "double bundle" Breeding Blanket concept left outboard segment, Fusion Eng. Des. 202 (2024) 114335.
[12] A. Quartararo, et al., Thermofluid-dynamic assessment of the EU-DEMO divertor single-circuit cooling option, Fusion Eng. Des. 188 (2023) 113408.
[13] H. Fenech, Heat Transfer and Fluid Flow in Nuclear Systems, Pergamon Press Inc., 1981.